Supporting Information

Unprecedented Family of Heterometallic Ln^{III}[18-Metallacrown-6] Complexes: Syntheses, Structures and Magnetic Properties

Wei Yang,[a] Hua Yang,[a] Su-Yuan Zeng,[a] Da-Cheng Li [a, b] and Jian-Min Dou *[a]
[a] Shandong Provincial Key Laboratory of Chemical Energy Storage and Novel Cell Technology, School of Chemical and Chemical Engineering, Liaocheng University, 252059 Liaocheng, P.R. China
[b] Institute of BioPharmaccutical Research, Liaocheng University, P.R. China

Contents:

lines are guides for the eyes.

Fig. S9 Temperature dependence of the in-phase (χ'_M) and out-of phase (χ''_M) ac susceptibility signals of **2** measured under 2.0 Oe field with a 1500 Oe dc field. The solid lines are guides for the eyes.

Fig. S10 Magnetization relaxation time ln(χ''/χ') vs T^{-1} plots for **2**. The solid line is fitted with the Debye model.

Fig. S11 Temperature dependence of the in-phase (χ'_M) and out-of phase (χ''_M) ac susceptibility signals of **3** measured under 2.0 Oe field with a zero dc field. The solid lines are guides for the eyes.

Fig. S12 Temperature dependence of the in-phase (χ'_M) and out-of phase (χ''_M) ac susceptibility signals of **3** measured under 2.0 Oe field with a 3000 Oe dc field. The solid lines are guides for the eyes.

Fig. S13 Magnetization relaxation time ln(χ''/χ') vs T^{-1} plots for **3**. The solid line is fitted with the Debye model.

Fig. S14 Temperature dependence of the in-phase (χ'_M) and out-of phase (χ''_M) ac susceptibility signals of **4** measured under 2.0 Oe field with a zero dc field. The solid lines are guides for the eyes

Table S1. Bond Valence Calculations (BVS) for complexes **1**−**4**

Table S2. Selected bond angles for **1**−**4**

Table S3. Measured $\Delta E_{\mathrm{eff}} / k_B$ and τ_0 values for **2** and **3**.

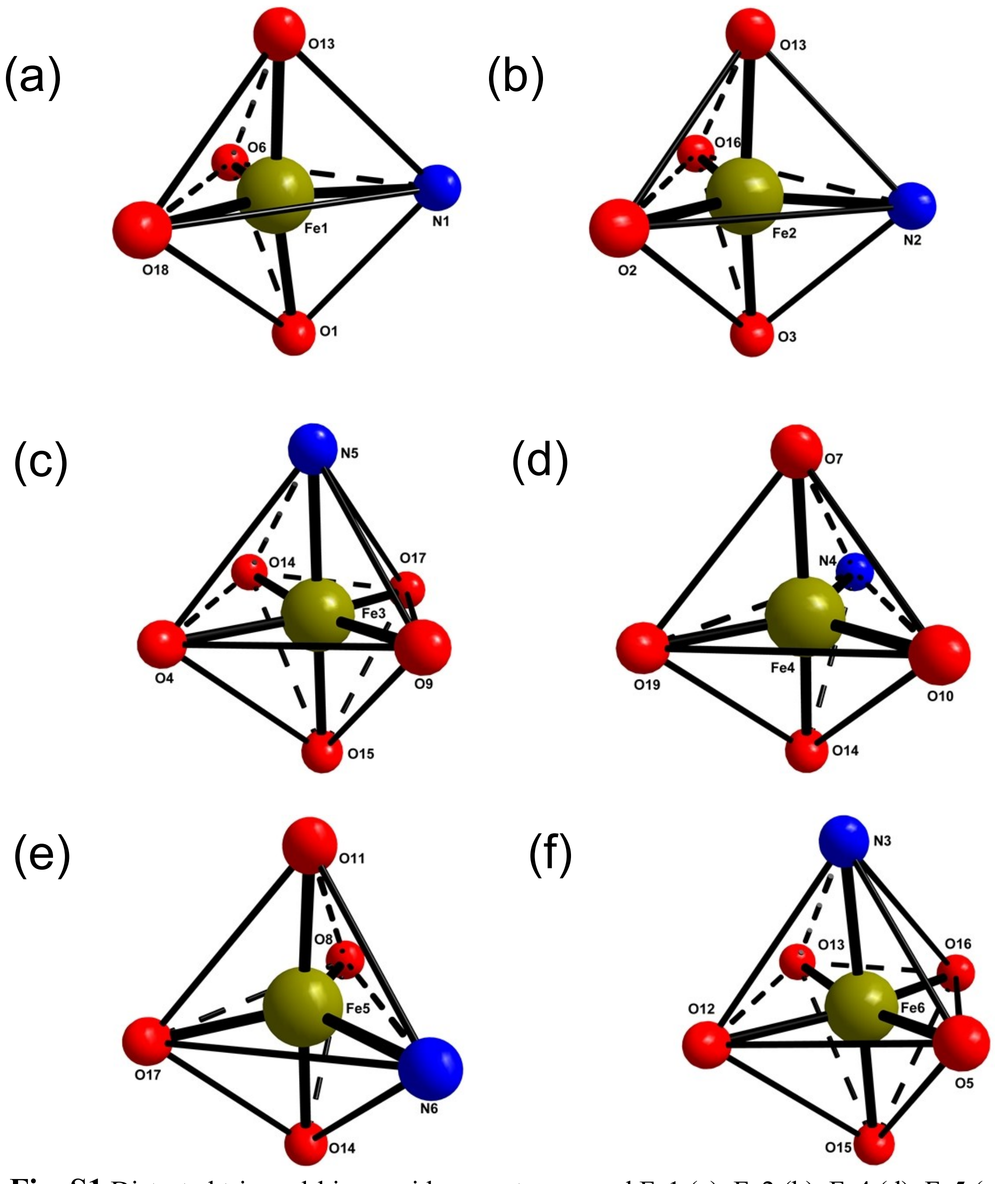

Fig. S1 Distorted trigonal-bipyramid geometry ground Fe1 (a), Fe2 (b), Fe4 (d), Fe5 (e) and distorted octahedral geometry around Fe3 (c), Fe6 (f) for complex **1**.

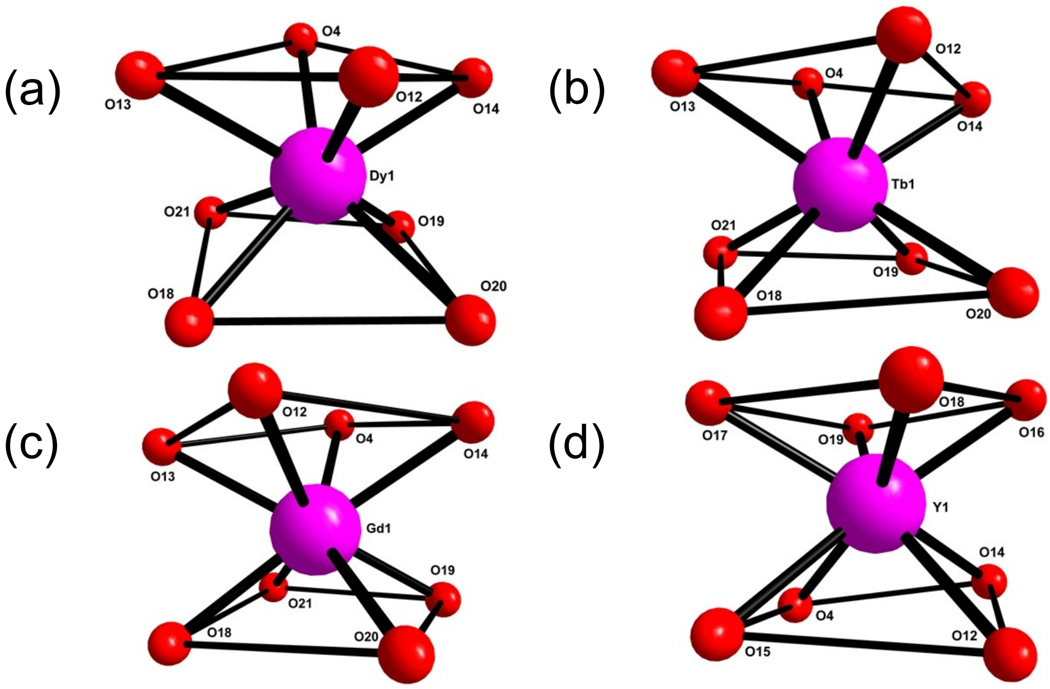

Fig. S2 Distorted square-antiprismatic geometries around Dy1 (a), Tb1 (b), Gd1 (c), Y1 (d)

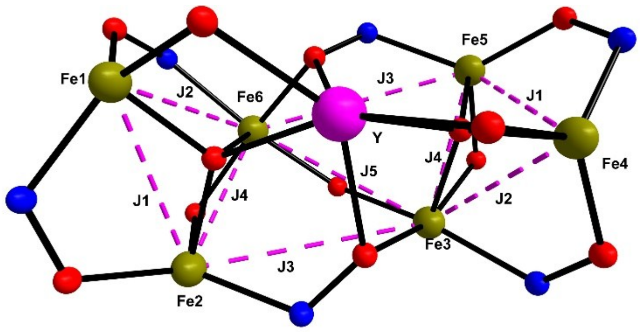

Fig. S3 The pairwise exchanging interaction in complex **4**

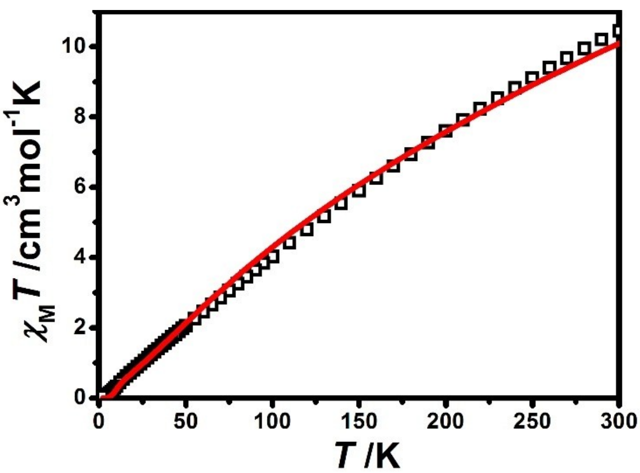

Fig. S4 $\chi_M T$ *vs* T plots for **4** at 1000 Oe. The solid line is the best fit according to the Hamiltonian given in eq 1.

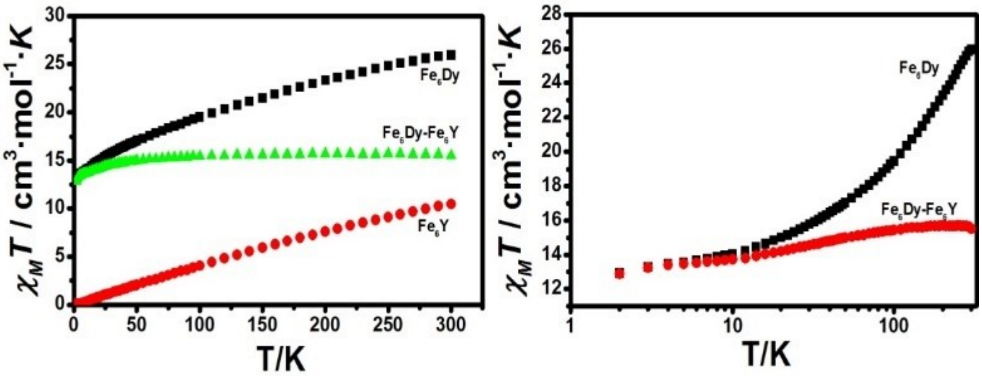

Fig. S5 Temperature dependence of the $\chi_M T$ product at 1000 Oe for complexes Fe_6Dy (**1**), Fe_6Y (**4**), and $\chi_M T$ (Fe_6Dy)–$\chi_M T$ (Fe_6Y) (left). The $\chi_M T$ plot of Fe_6Dy (**1**) and the substituted $\chi_M T$ plot (Fe_6Dy)–$\chi_M T$ (Fe_6Y) on logarithmic temperature scale (right).

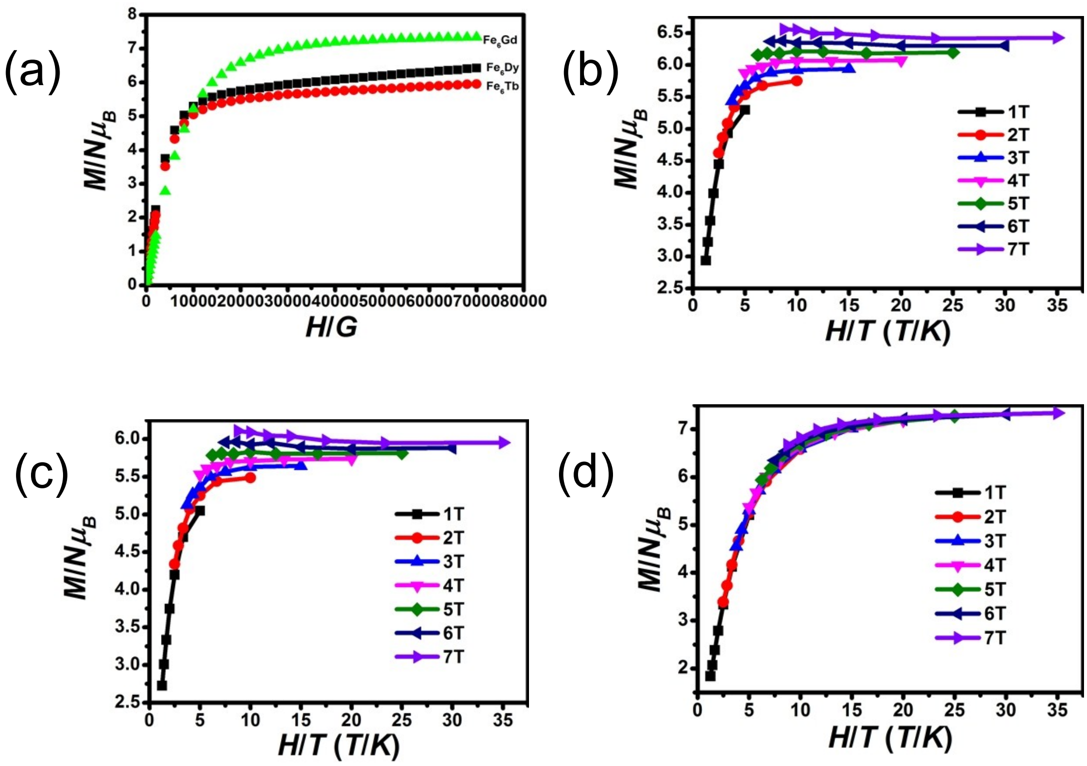

Fig. S6 Plots of isothermal magnetization *M* versus field *H* for **1**−**3** at 2 K (a). Field dependence of magnetizations of **1**(b), **2** (c), **3** (d)

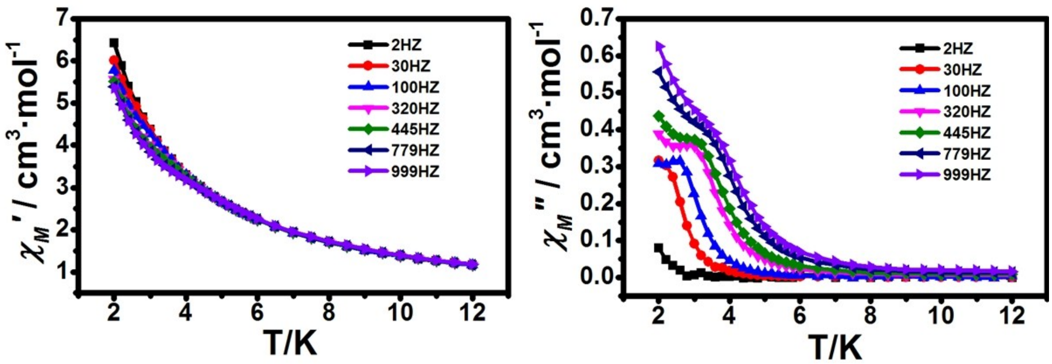

Fig. S7 Temperature dependence of the in-phase (χ'_{M}) and out-of phase (χ''_{M}) ac susceptibility signals of **1** measured under 2.0 Oe field with a zero dc field. The solid lines are guides for the eyes.

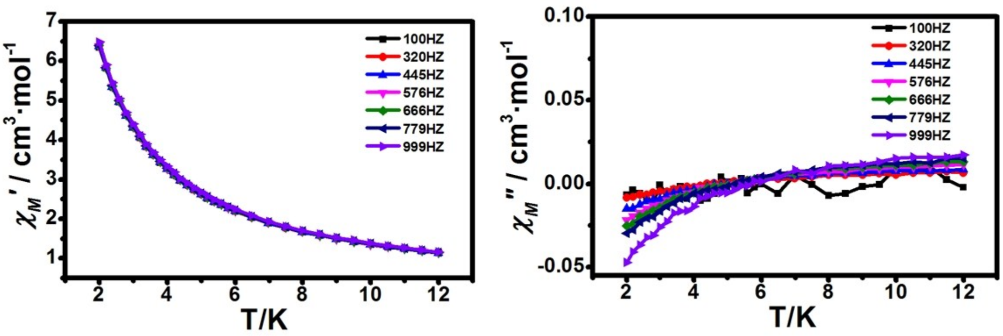

Fig. S8 Temperature dependence of the in-phase (χ'_{M}) and out-of phase (χ''_{M}) ac susceptibility signals of **2** measured under 2.0 Oe field with a zero dc field. The solid lines are guides for the eyes.

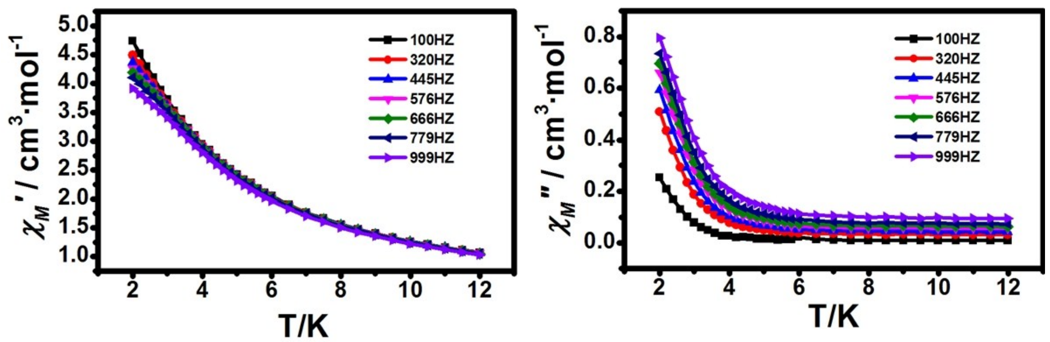

Fig. S9 Temperature dependence of the in-phase (χ'_{M}) and out-of phase (χ''_{M}) ac susceptibility signals of **2** measured under 2.0 Oe field with a 1500 Oe dc field. The solid lines are guides for the eyes.

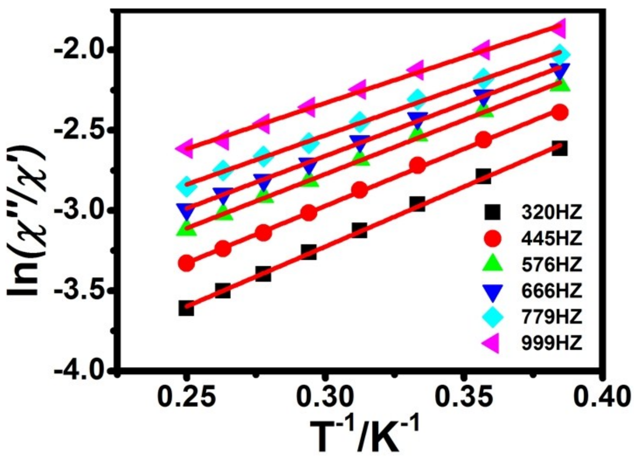

Fig. S10 Magnetization relaxation time ln(χ''/χ') vs T^{-1} plots for **2**. The solid line is fitted with the Debye model.

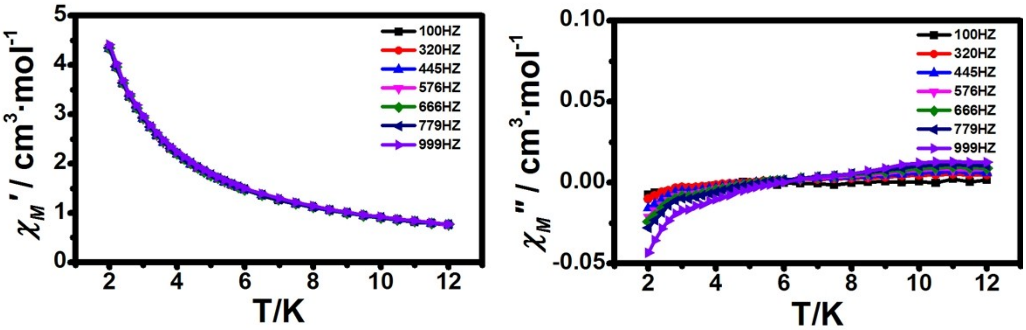

Fig. S11 Temperature dependence of the in-phase (χ'_{M}) and out-of phase (χ''_{M}) ac susceptibility signals of **3** measured under 2.0 Oe field with a zero dc field. The solid lines are guides for the eyes.

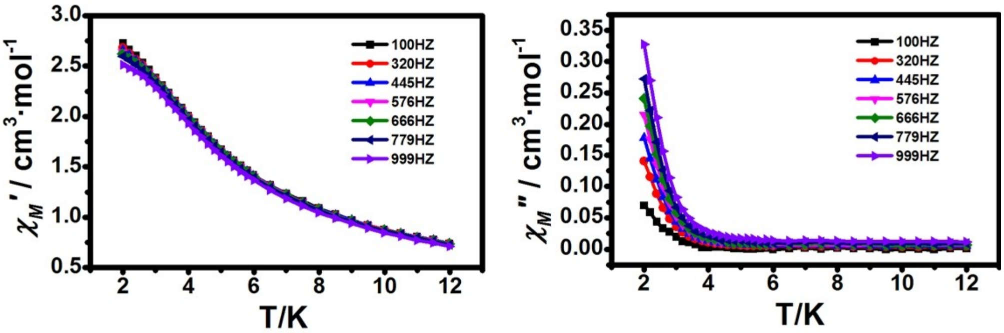

Fig. S12 Temperature dependence of the in-phase (χ'_{M}) and out-of phase (χ''_{M}) ac susceptibility signals of **3** measured under 2.0 Oe field with a 3000 Oe dc field. The solid lines are guides for the eyes.

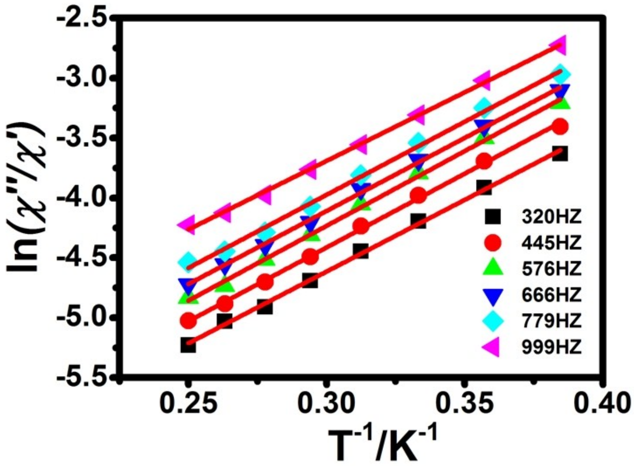

Fig. S13 Magnetization relaxation time ln(χ''/χ') vs T^{-1} plots for **3**. The solid line is fitted with the Debye model.

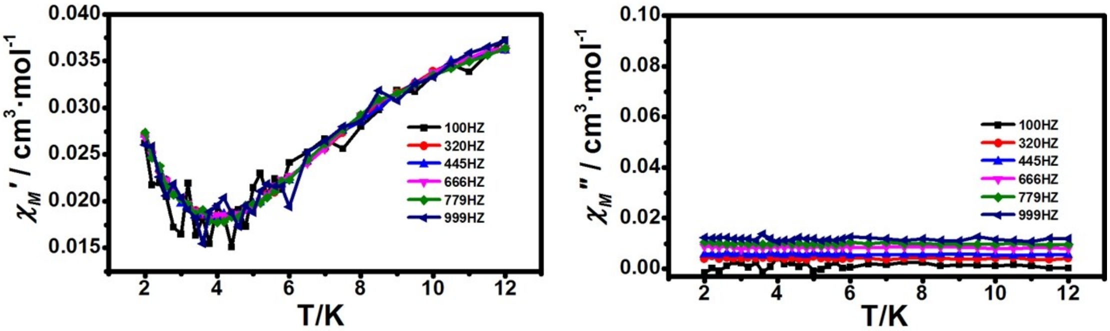

Fig. S14 Temperature dependence of the in-phase (χ'_M) and out-of phase (χ''_M) ac susceptibility signals of **4** measured under 2.0 Oe field with a zero dc field. The solid lines are guides for the eyes.

Table S1. Bond Valence Calculations (BVS) for complexes **1−4**

atom	Complex**1**		Complex **2**		Complex **3**		Complex **4**	
	+2	+3	+2	+3	+2	+3	+2	+3
Fe1	2.53	**2.99**	2.57	**3.04**	2.52	**2.99**	2.53	**2.99**
Fe2	2.60	**3.07**	2.60	**3.07**	2.60	**3.07**	2.60	**3.07**
Fe3	2.55	**3.01**	2.60	**3.07**	2.55	**3.02**	2.62	**3.10**
Fe4	2.56	**3.02**	2.61	**3.09**	2.56	**3.02**	2.60	**3.07**
Fe5	2.56	**3.03**	2.61	**3.09**	2.56	**3.03**	2.58	**3.05**
Fe6	2.54	**3.00**	2.57	**3.03**	2.54	**3.00**	2.54	**3.00**

Table S2. Selected bond angles for **1−4**

		1	
O(14)-Dy(1)-O(13) (γ angle)	117.87(13)	O(19)-Dy(1)-O(18) (γ angle)	114.65(16)
α angle (O14, O13)	59.93(13)	α angle (O19, O18)	57.32(16)
O(12)-Dy(1)-O(4) (γ angle)	101.17(14)	O(21)-Dy(1)-O(20) (γ angle)	127.48(16)
α angle (O12, O4)	50.58(14)	α angle (O21, O20)	63.73(16)
		2	
O(14)-Tb(1)-O(13) (γ angle)	117.96(12)	O(19)- Tb(1)-O(18) (γ angle)	115.88(14)
α angle (O14, O13)	58.98	α angle (O19, O18)	57.94
O(12)- Tb(1)-O(4) (γ angle)	101.28(12)	O(21)- Tb(1)-O(20) (γ angle)	127.82(16)
α angle (O12, O4)	50.64	α angle (O21, O20)	63.91
		3	
O(14)-Gd(1)-O(13) (γ angle)	117.8(2)	O(19)- Gd(1)-O(18) (γ angle)	116.2(3)
α angle (O14, O13)	58.90	α angle (O19, O18)	58.10
O(12)- Gd(1)-O(4) (γ angle)	100.1(3)	O(21)- Gd(1)-O(20) (γ angle)	128.2(3)
α angle (O12, O4)	50.05	α angle (O21, O20)	64.10
		4	
O(17)-Y(1)-O(16) (γ angle)	114.72(14)	O(15)- Y(1)-O(14) (γ angle)	118.07(12)
α angle (O17, O16)	57.36	α angle (O15, O14)	59.04
O(4)-Y(1)-O(12) (γ angle)	101.24(13)	O(18)- Y(1)-O(19) (γ angle)	126.75(14)
α angle (O4,O12)	50.62	α angle (O18, O19)	63.38

Table S3. Measured $\Delta E_{eff} / k_B$ and τ_0 values for **2** and **3.**

Frequency (Hz)	Complex **2**		Complex **3**	
	$\Delta E_{eff} / k_B$ (k)	τ_0 (s)	$\Delta E_{eff} / k_B$ (k)	τ_0 (s)
320	7.46	1.33×10^{-5}	11.96	8.56×10^{-7}
445	7.10	1.37×10^{-5}	12.31	6.78×10^{-7}
576	6.75	1.43×10^{-5}	12.47	5.98×10^{-7}
666	6.54	1.47×10^{-5}	12.18	6.37×10^{-7}
779	6.13	1.62×10^{-5}	12.19	6.22×10^{-7}
999	5.71	1.75×10^{-5}	11.44	8.06×10^{-7}